Nuclear Instruments and Methods in Physics Research B 129 (1997) 65–72

NIM B
Beam Interactions with Materials & Atoms

Optimisation and modelling of electrochemically etched polycarbonate track detectors

G. Vancraeynest, S. Franchoo, M. Huyse *, R. Moons

Instituut voor Kern- en Stralingsfysica, University of Leuven, Celestijnenlaan 200 D, B-3001 Leuven, Belgium

Received 5 December 1996; revised form received 3 March 1997

Abstract

Electrochemically etched polycarbonate nuclear track detectors have been used to detect the β-delayed α-decay of the ^{20}Na nuclei that were produced in the study of the astrophysically important ^{19}Ne(p,γ)^{20}Na reaction. The application required preceding investigations and developments. The insensitivity to β-radiation has been confirmed in off-line irradiations with β-sources up to doses of 20000 Gy. The density of intrinsic background tracks has been reduced to a mean value of 1.3 ± 0.1 cm^{-2}. The response function for α-detection as a function of energy and angle of incidence has been determined using Rutherford backscattered α-particles. A model for electrochemical etching that is generally valid for all ions and plastic detectors has been developed. It successfully reproduced the measured response function and track diameters.

PACS: 29.40.Wk; 81.60.Jw
Keywords: Makrofol; Electrochemical etching; Background reduction; Theoretical model

1. Introduction

Electrochemically etched (ECE) plastic nuclear track detectors have been used in radon dosimetry, geochemical exploration and geophysical monitoring of earthquakes for over a decade now [1,2]. Recently we have used ECE polycarbonate detectors in a nuclear physics experiment: the investigation of the astrophysically important ^{19}Ne(p,γ)^{20}Na reaction using a radioactive ^{19}Ne beam [3–5]. The produced ^{20}Na nuclei ($t_{1/2} = 448$ ms) were implanted in Al foils and brought in between consecutive pairs of track detectors, which registered the 2.15 MeV β-delayed α-branch (16.4%) in the decay of the ^{20}Na activity.

The requirements for the successful application of track detectors in our experiments were: (i) strict insensitivity to the huge β^+-background ($E_{max} = 2.2$ MeV) coming from the radioactive ^{19}Ne beam ($\sim 10^9$ pps, $t_{1/2} = 17.2$ s); (ii) low intrinsic background, i.e. the tracks that appear on unused detectors, because of the low expected reaction yields; (iii) reliable determination of the detection effiency and (iv) clear track development in order to facilitate the search for only a few tracks per cm^2.

The last requirement is nicely fulfilled using electrochemical etching. In this article we report on the research and development to achieve the other goals, using ECE plastic track detectors. Tests on the insensitivity to β-radiation are discussed in Section 2. The reduction of the intrinsic background level is treated in Section 3. The response function for α-detection was determined experimentally and a theoretical and generally valid model for ECE that nicely reproduced the observed response function and the corresponding track diameters is presented in Section 4. In Section 5 we briefly summarise and indicate the relevance of our results towards more classical applications of ECE plastic track detectors.

The detector foils were 300 μm thick polycarbonate foils (Makrofol E) that were electrochemically etched by the Studiecentrum voor Kernenergie at Mol, Belgium using their standard etch conditions [6]. The etching solution consists of a mixture of ethyl alcohol and a 6N KOH solution with a volume ratio of 1:4 at 25°C. The bulk etch velocity v_b equals 0.5 μm/h. After 30 min pre-etching an alternating voltage of 800 V effective at 2 kHz is applied over the foils during 3 h. The detector foils are dried in air

* Corresponding author. Fax: +32-16-327-985; email: mark.huyse@fys.kuleuven.ac.be

PII S0168-583X(97)00162-6

and ECE-tracks counted by means of a micro-fiche reader or a microscope.

2. Insensitivity to β-radiation

The positron flux from the implanted beam that was received by the first detector pair in our $^{19}Ne(p,\gamma)^{20}Na$ measurements amounted up to 4×10^{12} cm^{-2}. Calculating the stopping of the positrons at the mean energy in the ^{19}Ne decay of 938 keV the corresponding dose is estimated to be 1200 Gy. In a preceding series of off-line irradiations with ^{18}F and $^{90}Sr/^{90}Y$ sources, up to a dose of 20000 Gy, we investigated if the detectors were indeed completely insensitive to β-radiation, i.e. that they do not develop ECE-tracks and that their *chemical* etching behaviour is not affected. The observed density of ECE-tracks on the irradiated detectors did not differ from the background values on control detectors and the bulk etch velocity for chemical etching was not influenced, indicating that the properties under chemical etching remains unchanged. These observations are consistent with the results in [7].

3. Reduction of the intrinsic background

At the low signal that was to be measured it was crucial to make the intrinsic background as small as possible. The Intrinsic Background Level (IBL) of a detector is determined by its history. Three sources of intrinsic background are to be considered: (i) the α-decay of ^{222}Rn, that is present in the air, and its daughters; (ii) radioactive contaminants in the detector material itself and (iii) water inclusions. Therefore the IBL differs from batch to batch. The detectors that were used in the experiments came from a batch with a mean IBL of 13.2 ± 0.4 cm^{-2}.

Following Schmitz [8] a substantial reduction of this figure down to 2.9 ± 0.2 cm^{-2} was achieved by annealing them at 120°C under atmospheric circumstances during 3 days prior to the experiment. It is believed that annealing eliminates (the majority of) the water inclusions. It was explicitly checked that the annealing did not change the properties of the detector foils under chemical or electrochemical etching.

The remaining background tracks were studied under a microscope with polarised light. When compared with genuine α-induced ECE-tracks some of the background tracks look quite different (Fig. 1): the channel leading to the tree-like structure in the bulk is broad and irregular for some background tracks whereas it is always very fine in the case of α-induced tracks. This distinction led to a supplementary reduction of the intrinsic background to a mean level of 1.3 ± 0.1 cm^{-2}. We surmise that the background tracks with a broad entrance channel are due to water inclusions that have migrated towards each other.

4. The response function for α-detection

4.1. Experimental determination

The response function for α-detection, i.e. the detection efficiency as a function of energy and angle of incidence of the α-particle, was determined experimentally using Rutherford backscattered (RBS) helium beams. The backscattered α-beam energy and intensity was measured with a Si-diode detector. In Fig. 2 the results are presented. The full dots are our data points. The error on the efficiency resulted from the statistical uncertainties on the number of counts on the track detectors and in the normalisation spectrum and the systematical uncertainty on the experimental geometry. Also included in Fig. 2 are data points at normal incidence of Vanmarcke et al. [6] (open dots).

4.2. A theoretical model for electrochemical etching

In order to understand the observed α-detection efficiencies and to complete the response function for α-detection, we developed a theoretical model for ECE. Its validity however is not restricted to α-particles and, after proper recalibration of its free parameters, even not to the specific etching procedure or detector material.

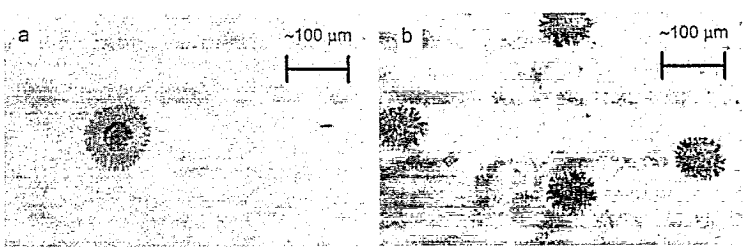

Fig. 1. ECE-tracks viewed under a microscope (× 100) using polarised light: (a) an intrinsic background track, (b) a genuine α-induced track.

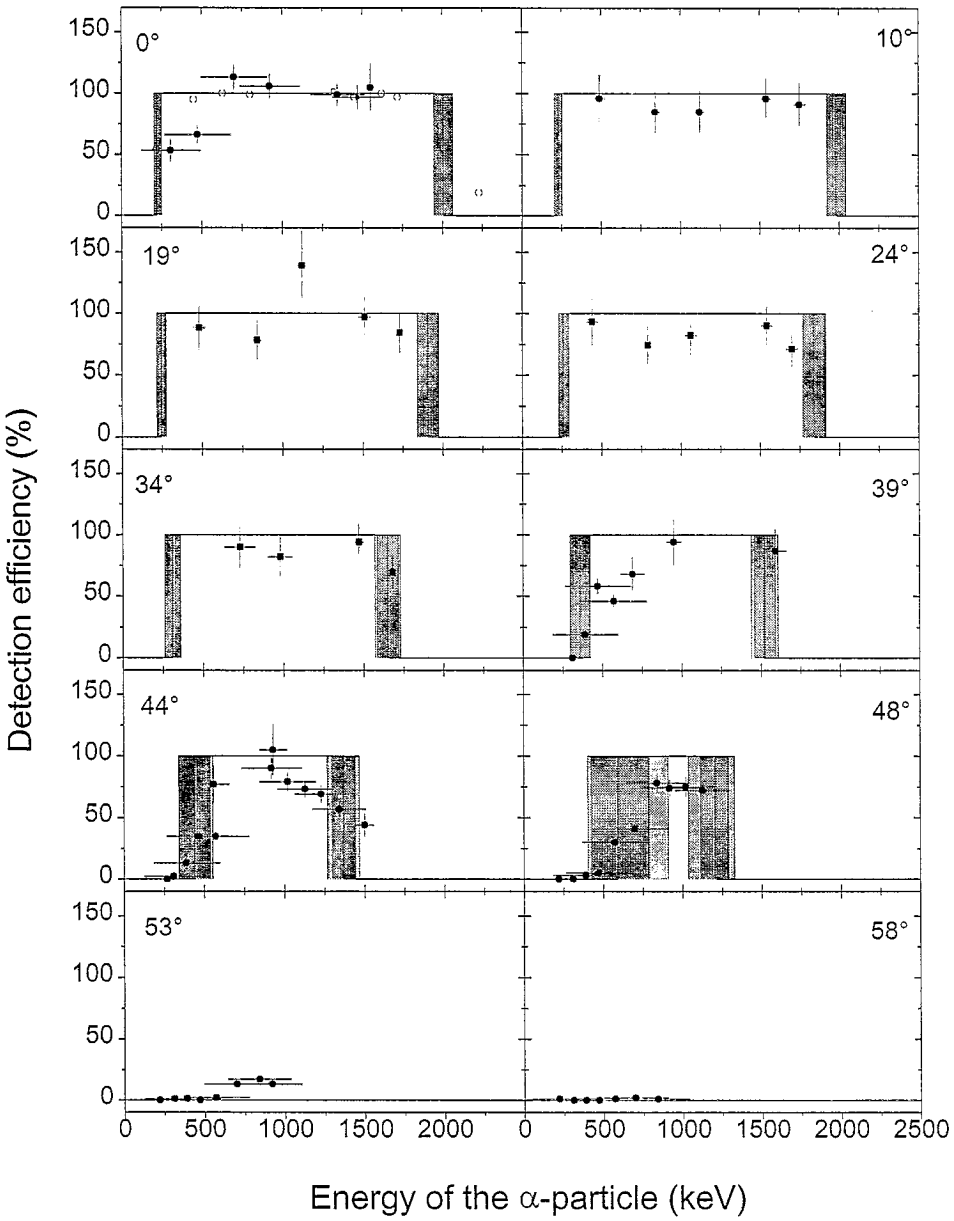

Fig. 2. Efficiency for detection of α-particles as a function of energy of incidence at various angles of incidence. Open dots: Vanmarcke et al. [6], full dots: this work. The horizontal bars indicate the energy spread of the α-particles at incidence. The full lines are the sensitive energy windows calculated by our theoretical model. The dark grey hatching gives the uncertainty on the position of the borders due to the uncertainty on the fitted parameters of the model. The light grey hatching in addition incorporates the uncertainty (2°) on the nominal value of the angle of incidence.

4.2.1. Basic ideas

A chemical etched (CE) track is formed when the latent track of a charged particle is exposed to a chemical etchant. When a voltage is applied over the detector enormous electric fields result at the tip of the CE-track. CE keeps taking place until the field at the tip, E, exceeds the

critical value for breakdown E_{crit} which is 230 kV/mm for polycarbonate [9]. This we call the ECE-criterion:

$$E \geq E_{crit}. \tag{1}$$

The combination of local extreme electromechanical stress and the action of the etchant gives rise to a tree-like structure: the ECE-track. The ECE-track continues to grow until the end of the etching procedure at a constant rate, called the electrochemical etch velocity v_{ECE}. The sooner the breakdown occurs, the bigger the eventual ECE-track.

Often Mason's equation [10] is used to calculate the field at the tip of the CE-track. However, as was pointed out by Pitt et al. [11], this equation is only valid if the length L of the CE track is not much smaller than the thickness D of the detector and this is not the case for most applications of ECE. The equation that is to be used is Smythe's equation [12] which holds for if $D \gg L \gg R$ (R is the radius of the track at the tip). Smythe's equation was extended for slant incidence in [13] and, writing the time dependencies explicitly, the field at the tip of the CE-track is given by:

$$E(t) = \frac{U}{D(t)} \frac{2\dfrac{L(t)\cos\theta}{R(t)}}{\ln\left(4\dfrac{L(t)\cos\theta}{R(t)}\right) - 2} \quad (R \ll L \ll D). \tag{2}$$

U is the amplitude of the voltage applied over the detector and θ is the angle of incidence with respect to the normal of the particle. The thickness $D(t)$ is given by

$$D(t) = D(t=0) - v_B t.$$

Here v_B is the bulk etch velocity. The parameters $L(t)$ and $R(t)$ are given by the geometry of the CE-track at time t.

We used the well-known formalism of Somogyi et al. [14], that describes the geometry of the CE-track during the course of the etching in terms of the etching response $V \equiv v_T/v_b$, with v_T the track etch velocity, as a function of the residual range. In [15] V has been parametrised in

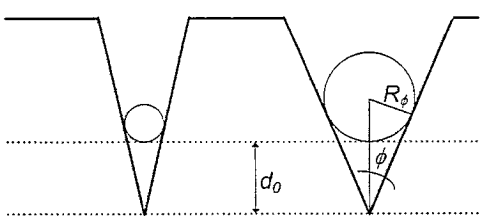

Fig. 3. Representation of the geometrical model of Al-Najjar et al. [18] of the effective radius at the top of a CE-track for ECE.

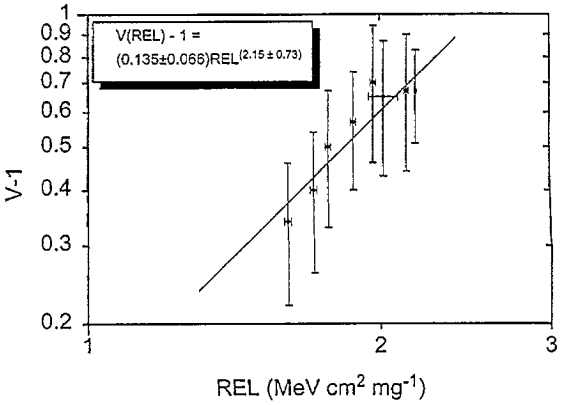

Fig. 4. Relative etching response $(V-1)$ as a function of Restricted Energy Loss. The full line is a fit of the parameters α and β of Eq. (3). The horizontal error bars correspond to the spread on the energy of the α-particles at incidence.

terms of the Restricted Energy Loss (REL), which is a measure of the *density* of the damage along the latent track:

$$V = 1 + \alpha \mathrm{REL}^{\beta}. \tag{3}$$

The threshold energy for secondary electrons adopted in the calculation of the REL is 1 keV [15,16]. The parameters α and β depend on the detector material and the etch conditions and we have determined them in a separate series of measurements (Section 4.2.2). Using the TRIM values [17] for the range of the charged particle we then could express V as a function of the residual range.

In the formalism of Somogyi et al. [14], the region of enhanced etchability in the track is assumed to be limited to a very narrow, highly damaged central zone, in other words: the track etch velocity is along the track without radial component. By consequence these ideal tracks have a zero radius at their tip. Al-Najjar et al. [18] have proposed a simple geometrical model that relates the effective radius R at the top for ECE to the opening angle ϕ of the CE-track. This is plausible indeed: the bigger the opening angle, the bigger the radius at the top. They proposed a linear relation between the effective radius at the top and the radius R_ϕ of an imaginary sphere located at a fixed distance d_0 from the top (Fig. 3):

$$R = A + R_\phi = A + d_0\rho \quad \text{with } \rho \equiv \frac{\sin\phi}{1-\sin\phi}. \tag{4}$$

According to [18] the parameter d_0 is related to the fact that the very top of the CE-track does not act as a sparking point because it is filled with etch products and not with the conducting etchant. In Section 4.2.3 we describe how we determined the parameters A and d_0.

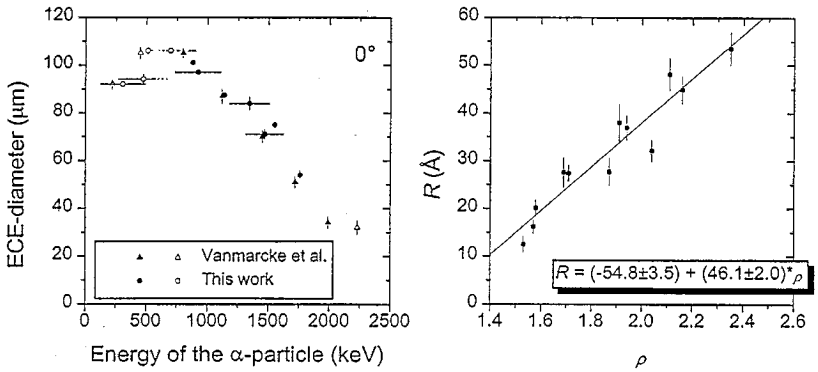

Fig. 5. Left: the mean diameter of α-induced ECE-tracks at normal incidence as a function of the energy of the α-particle. The horizontal bars indicate the energy spread of the α-particles at incidence. Only the data points indicated by full symbols were used to determine the parameters A and d_0 of Eq. (4). Right: determination of the parameters A and d_0 of Eq. (4) (see text).

4.2.2. The etching response V

The etching response was determined by comparing the diameters of α-induced CE-tracks, d_α, and of tracks induced by fission fragments from a ^{252}Cf source, d_{fission}. The detectors were chemically etched using the etching solution described in Section 1. The etching time was kept short (one hour), so that only a small portion of the latent α-induced tracks was etched: 0.5 to 0.8 μm depending on the energy of incidence which ranged from 150 keV to 1900 keV. Consequently v_T could be considered constant. For the fission fragments the track etch velocity is much bigger than the bulk etching velocity. The etching response V_α over the etched portion of the α-induced track then follows from:

$$V_\alpha = \frac{1 + \left(\frac{d_\alpha}{d_{\text{fission}}}\right)^2}{1 - \left(\frac{d_\alpha}{d_{\text{fission}}}\right)^2}.$$

The CE-track diameters were measured with a scanning electron microscope (JEOL-JSM6400) at magnifications from 30000 to 90000. The magnification was checked to be perfectly linear. Per energy we measured about ten tracks. A 0.04 μm systematical uncertainty which incorporates the sensitivity to the SEM imaging parameters was quadratically added to the statistical uncertainty (typically 5% or ~ 0.02 μm).

For each energy of incidence the REL was calculated and $V_\alpha - 1$ was plotted bilogaritmically against the REL values expressed in MeV.cm^2/mg (Fig. 4). The fitted parameters of Eq. (3) are $\alpha = (0.135 \pm 0.07)$ MeV^{-1} cm^{-2} mg and $\beta = 2.2 \pm 0.7$. This compares to $\alpha = 0.096$ MeV^{-1} cm^{-2} mg and $\beta = 2.82$ in [15] for the same detector material and over a broader range of REL values, but for different etch conditions. The parametrisation of the etching response in our etch conditions was determined with α-particles and is therefore only reliable for light particles.

4.2.3. The effective radius at the top of the CE-track for ECE

In the left part of Fig. 5 the mean diameters of ECE-tracks of normally incident α-particles are displayed as a function of the energy of incidence. They range from 32 to 106 μm, corresponding to the initiation of the treeing at the end of the etching procedure or right after the application of the alternating voltage, respectively. Apparently 32 μm is the minimum value for an ECE-track. The value for v_{ECE} that was deduced is 24.7 μm/h and it was used to calculate the time of initiation of the treeing t_{ECE} from the observed diameters of the ECE-tracks.

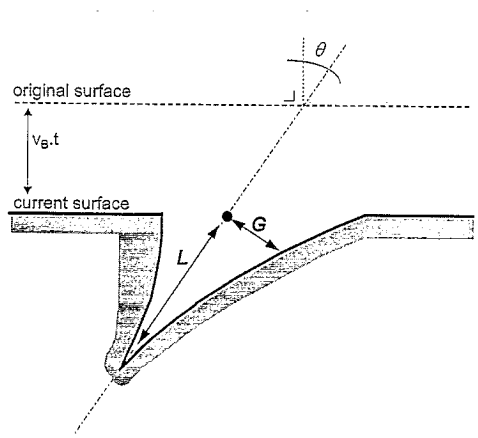

Fig. 6. Section along the major axis of the elliptic opening of a CE-track induced by a particle at slant incidence. Distances G and L are used to determine the mean opening angle.

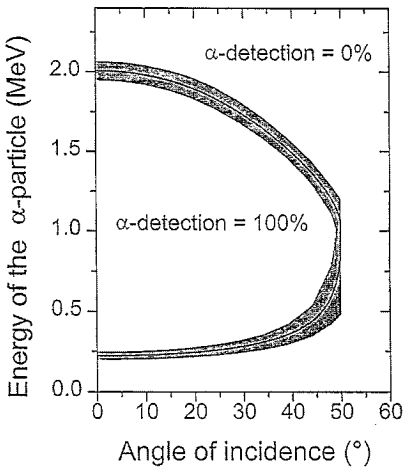

Fig. 7. Theoretical response function for α-detection. The dark grey hatching represents the uncertainty due to the uncertainty on the fitted parameters of the model.

Between 0.25 and 0.8 MeV the ECE-tracks have developed immediately, which means that the ECE-criterion, Eq. (1), was a strict inequality at the time the voltage was applied. Therefore the 12 data points with smaller diameters at the high energy side indicated by full dots in Fig. 5 were used to determine the effective radius R at the tip for ECE: we first determined t_{ECE}, then we calculated the geometry of the CE-track (length L, diameter of the opening, opening angle at the top, ...) at $t = t_{ECE}$ and finally solved *equality* (1) for R. We then calculated the quantity ρ of Eq. (4) for each CE-track using a mean opening angle $\phi = \arctan(diameter/2L)$. Using the opening angle at the top in stead resulted in serious deviations from a linear relation between ρ and R in the cases that the top was over the Bragg peak (convex top). The results are plotted in the right part of Fig. 5. The R-values are in the order of what is expected for the radial dimension of latent tracks, which shows that our approach is physically sensible. The data points were nicely fitted by a straight line:

$$R\,(\text{Å}) = (-54.8 \pm 3.5) + (46.1 \pm 2.0) * \rho$$

In the case of slant incidence the axial symmetry of the CE-track is broken and a mean opening angle can be defined in more than one way. For slant incidence we had at our disposal 24 measurements from our determination of the response function for α-detection (Section 4.1) in which the mean diameter was less than 106 μm. Using the parameters determined for normal incidence we calculated the ECE diameters. The deviation from the observed values ($\chi^2 = 1.5$ p.d.f.) was smallest if the mean opening angle was calculated in the plane formed by the track axis and the major axis of the elliptic opening at the point where the track axis crosses the current detector surface (Fig. 6): $\phi = \arctan(G/2L)$.

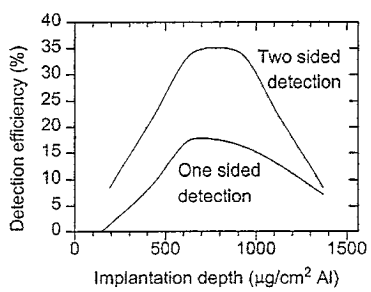

Fig. 8. The efficiency for detecting the 2.15 MeV α-particles in the decay of the implanted ^{20}Na activity as a function of implantation depth in the 1.56 mg/cm^2 Al implantation foil.

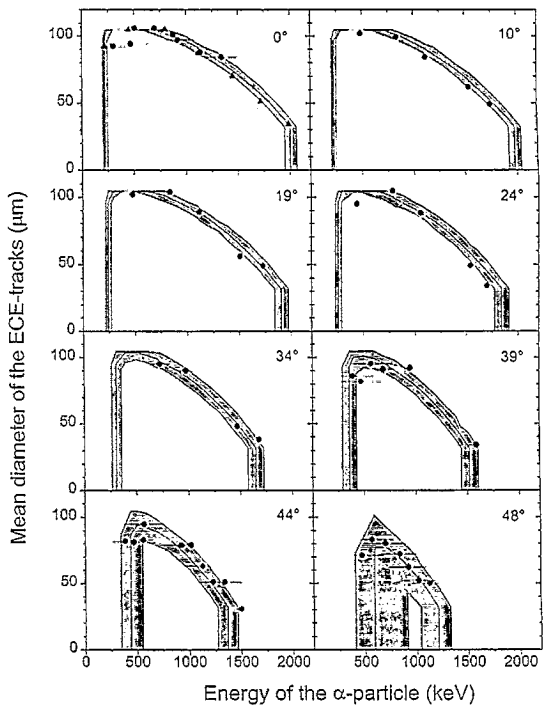

Fig. 9. Mean diameters of α-induced ECE-tracks as a function of energy of incidence at various angles of incidence. Triangles: Vanmarcke et al. [6]; circles: this work. The horizontal bars indicate the energy spread of the α-particles at incidence. The full lines are the diameters calculated by the theoretical model. The light hatching incorporates the uncertainty on the fitted parameters of the model and the uncertainty (2°) on the nominal value of the angle of incidence.

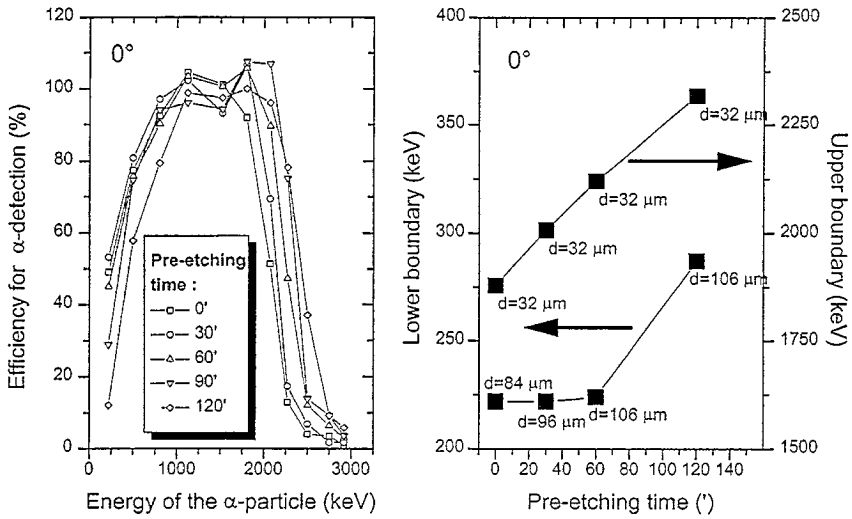

Fig. 10. Left: efficiency for the detection of α-particles as a function of energy at normal incidence for different pre-etching times [19]. Right: position of the lower and upper boundaries of the sensitive energy window for detection of α-particles at normal incidence as a function of pre-etching time calculated with the model. At each data point the calculated diameters of the ECE-tracks are given.

4.2.4. A FORTRAN program

For a given particle (A,Z) with a given energy and angle of incidence, the program calculates the geometry of the CE-track and the effective radius at the top as a function of the etching time. When the ECE-criterion, Eq. (1), is fulfilled, the program leaves the loop and calculates the diameter of the eventual track using v_{ECE}.

If during the etching time the ECE-criterion is never met, the loop ends and the program reports that no ECE-track has been developed. If the end of the latent track is reached before the end of the etching without having fulfilled the ECE-criterion, treeing will not occur at later times because the CE-track gets blunt and transforms into a shallow and broad cavity. The program quits the loop reporting no ECE occurred.

4.2.5. Results

In Fig. 2 the full lines indicate the sensitive energy windows for α-detection calculated with the model. The correspondence between experiment and theory is good. The model succeeds in reproducing the narrowing of the sensitive energy window with bigger angles of incidence up to the disappearance at 50°. In Fig. 7 the theoretical response function for α-detection, which is a block function in our model, is represented in the (E,θ)-plane.

Using our theoretical model the effective detection efficiency for the 2.15 MeV β-delayed α-particles emitted by the ^{20}Na nuclei in the ^{19}Ne(p,γ)^{20}Na measurements was calculated as a function of their implantation depth in the Al implantion foil (Fig. 8). When the implantation foil is sandwiched in between two detectors a broad plateau shows up around the middle of the implantation foil. Since in our measurements the ^{20}Na activity was always implanted at about the middle of the foil thanks to a preceding degrader foil with appropriate thickness, the determination of the effective detection efficiency can be considered as reliable.

The model also nicely reproduced the diameters of the ECE-tracks on the detectors that had been used in the determination of the response function for α-detection (Fig. 9). We notice that the smaller diameters at low energies is a real effect: for low energy α-particles the top of the CE-track is already over the Bragg peak when the voltage is applied. The top is convex and the CE-track has to grow a bit further in order to meet the ECE-criterion. As a result the treeing is delayed and smaller ECE-track are developed eventually. On the other hand, if the α-particle had a high energy, then the etching takes place considerably before the Bragg peak and the CE-track has to grow some time before the ECE-criterion is fulfilled, again resulting in smaller ECE-tracks. At the high energy end of the sensitive energy window the treeing takes place only at the very end of the etching procedure, so that the diameter is minimal (32 μm). The distribution of diameters of ECE-tracks on a detector can in some sense be considered as an energy spectrum.

To test our understanding of the ECE process explicitly, we checked if our model could reproduce the influence of the pre-etching time (i.e. the chemical etching before the voltage is applied) on the sensitive energy

window and on the diameters of the ECE-tracks. The left part of Fig. 10 shows experimentally determined sensitive energy windows for pre-etching times from 0 up to 120 min for normal incidence [19]. At the right the borders of the sensitive energy window together with the diameter of the ECE-tracks at the border calculated by our model are shown in function of the pre-etching time. The time during which the voltage was applied was kept constant at 3 h. The experimental observations are reproduced indeed.

5. Conclusion

In addition to the well known use of chemically etched track detectors in nuclear physics, electrochemically etched polycarbonate detectors have now been employed in a nuclear physics experiment. This triggered technical and scientific development concerning this type of detectors leading to a considerable background reduction down to a density of 1.3 ± 0.1 cm^{-2} and the development of a theoretical and generally valid model for electrochemical etching.

The model is conceptually simple and, although only twelve data points at normal incidence have been used for the determination of its free parameters, it succeeded in reproducing the detection efficiency and the track diameters at all angles and energies. The model does not take into account statistical effects, which probably cause the response function for α-detection not to be a sharp defined block function. Nor has the dependency on the frequency of the alternating voltage been incorporated. The model is in principle valid for the ECE of latent tracks of all kinds of ions and after recalibration of its free parameters is applicable to other detector materials (e.g. CR-39) and other etch conditions. Therefore we hope that it may contribute in the optimisation of ECE plastic detectors in other fields of applications, radon dosimetry in particular. Moreover, the reduction of the intrinsic background level may lead to a substantial enhancement of the sensitivity of the latter application.

Acknowledgements

The authors would like to thank Dr. H. Vanmarcke and P. Willeborts for etching the detectors at the SCK, Mol, Belgium, Ir. J. Schmitz, Kf Karlsruhe, Germany, Prof. W. Enge, Kiel, Germany and Ir. E. Ferrain, UCL, Belgium for useful discussions and Prof. R. Swennen and Prof. W. Viane, KUL, Belgium for assistance in microscopy. G.V. was at the time Research Assistent of the NFWO, Belgium. S.F. is Research Assistent of the NFWO, Belgium. This work presents research results of the Belgian Programme on Interuniversity Poles of Attraction initiated by the Belgian Federal Services of Scientific, Technical and Cultural Affairs and was also supported by a grant from the National Fund of Scientific research of Belgium (project nr. 2.0038.9).

References

[1] S.A. Durrani and R.K. Bull, Solid State Nuclear Track Detection (Pergamon Press, Oxford, 1987), and references therein.
[2] R.L. Fleischer, MRS Bull. 20 (1995) 35.
[3] R.D. Page et al., Phys. Rev. Lett. 73 (1994) 3066.
[4] C. Michotte et al., Phys. Lett. B 381 (1996) 402.
[5] G. Vancraeynest et al., Proc. 4th Int. Conf. on Radioactive Nuclear Beams, Omiya, 4–7 June 1996, ed. S. Kubono, Nucl. Phys. A, to be published .
[6] H. Vanmarcke, A. Janssens, Nucl. Tracks 12 (1986) 689.
[7] A.N. Goland, E. der Mateosian, Nucl. Instr. and Meth. 106 (1973) 295.
[8] J. Schmitz, Haubtabteilung Sicherheit, (Kernforschungszentrum, Karlsruhe, Germany), private communication.
[9] H. Saechtling, Kunststoff—Taschenbuch (Carl Hanser Verlag, München, 1979).
[10] J.H. Mason, in: Progress in Dielectrics, Vol. 1, eds. J.B. Birks and J.H. Schulman (Heywood, London, 1959), bottom of page 17; J.H. Mason, Proc. Inst. Elect. Engrs. 98 (1951) 44, Eqs. (10) and (11).
[11] E. Pitt, B. Werner, Kerntechnik 52 (1988) 126.
[12] W.R. Smythe, Static and Dynamic Electricity (McGraw-Hill, New York, 1939) pp. 168–169; J.H. Mason, Proc. Inst. Elect. Engrs. 98 (1951) 44, Eq. (8).
[13] E. Pitt, A. Scharmann, R. Simmer, Nucl. Tracks Radiat. Meas. 19 (1991) 517.
[14] G. Somogyi and S.A. Szalay, Nucl. Instr. and Meth. 109 (1973) 211; G. Somogyi, Nucl. Instr. and Meth. 173 (1980) 21.
[15] G. Somogyi, K. Grabisch, R. Scherzer, W. Enge, Nucl. Instr. and Meth. 134 (1976) 129.
[16] E.V. Benton, W.D. Nix, Nucl. Instr. and Meth. 67 (1969) 343.
[17] F.J. Ziegler, J.P. Biersack and U. Littmark, The Stopping and Ranges of Ions in Matter, Vol. 1 (Pergamon, New York, 1985).
[18] S.A.R. Al-Najjar, S.A. Durrani, Nucl. Tracks 12 (1986) 37.
[19] H. Vanmarcke, Ph. D. Thesis, Rijksuniversiteit Gent, Belgium (1987), unpublished.